Inorg. Chem. **2009**, *48*, 3257−3267

Structural Study of Ga(III), In(III), and Fe(III) Complexes of Triaza-Macrocycle Based Ligands with N_3S_3 Donor Set

Johannes Notni,*,† Karolin Pohle,‡ Joop A. Peters,‡ Helmar Görls,§ and Carlos Platas-Iglesias||

Department of Nuclear Medicine, Technische Universität München, Ismaninger Strasse 22, D-81675 München, Germany, Laboratory of Biocatalysis and Organic Chemistry, Department of Biotechnology, Delft University of Technology, Julianalaan 136, 2628 BL Delft, The Netherlands, Institut für Anorganische and Analytische Chemie, Friedrich-Schiller-Universität Jena, Lessingstrasse 8, D-07743 Jena, Germany, and Departamento de Química Fundamental, Campus da Zapateira, Universidade da Coruña, Alejandro de la Sota 1, 15008 A Coruña, Spain

Received January 20, 2009

Two new ligands, 1,4,7-tris(2-mercaptoethyl)-1,4,7-triazacyclodecane (**L2**) and 9-methyl-1,4,7-tris(2-mercaptoethyl)-1,4,7-triazacyclodecane (**L3**), have been synthesized by reaction of the free triazacycloalkanes with ethylene sulfide. Complexes of **L2** with Ga(III), In(III), and Fe(III), as well as Ga(III) and In(III) complexes of **L3**, have been characterized by single crystal X-ray diffraction. In all cases, the metal ions are coordinated in a trigonal-antiprismatic environment with varying degrees of distortion. **L2** complexes are isostructural and exhibit the *chair*-$\Delta(\lambda\lambda)(\delta\delta\delta)$ conformation, whereas Ga**L3** and In**L3** adopt *twist-boat*-$\Delta(\lambda\lambda)(\delta\delta\delta)$ and *twist-boat*-$\Delta(\lambda\lambda)(\lambda\delta\delta)$ configurational isomers and their enantiomers, respectively. In addition, we report the cystal structure of the Fe(III) complex of the known ligand 1,4,7-tris(2-mercaptoethyl)-1,4,7-triazacyclononane (TS-TACN, **L1**), which is isostructural to its Ga(III) and In(III) complexes. All aforementioned complexes are compared (including literature data of Ga(TS-TACN) and In(TS-TACN)), and the influence of ring size and backbone substitution on coordination geometries is discussed. Furthermore, the solution structures of Ga(III) and In(III) complexes of the new ligands have been investigated employing NMR spectroscopy and density functional theory (DFT) calculation. The latter revealed that for all compounds, the most stable structures are those where the six-membered chelate ring adopts chair conformation. NMR measurements confirmed this proposal for the **L2** complexes. In contrast, the Ga**L3** complex is present as a mixture of chair and twist-boat isomers. This implies that for this complex, interconversion between both forms is occurring, which necessarily includes intermediate partial decoordination of the metal ion. **InL3** occurs as a single species, but an unambiguous determination of its conformation was not possible.

Introduction

Metal complexes have been in use in the field of medical imaging for decades, the most prominent examples being the application of gadolinium in magnetic resonance imaging (MRI)[1−3] and ^{99m}Tc in radioimaging (gamma scintigraphy, single photon emission computed tomography (SPECT)).[4] Apart from these well-known examples, complexes of indium and gallium radioisotopes are useful for nuclear imaging. Cyclotron-produced ^{111}In and ^{67}Ga are γ-emitters with half-lives of 62 and 78 h, respectively, that are widely used in gamma scintigraphy.[5] ^{68}Ga, a β^+ emitter with a half-life of ≈68 min, is a promising candidate for application in positron emission tomography (PET). It is a generator nuclide which means that no on-site cyclotron is needed at PET facilities.

* To whom correspondence should be addressed. E-mail: johannes.notni@tum.de.
† Technische Universität München.
‡ Delft University of Technology.
§ Friedrich-Schiller-Universität Jena.
|| Universidade da Coruña.

(1) Caravan, P.; Ellison, J. J.; McMurry, T. J.; Lauffer, R. B. *Chem. Rev. (Washington, DC, U.S.)* **1999**, *99*, 2293–2352.
(2) Merbach, A. E.; Tóth, E. *The Chemistry of Contrast Agents in Medical Magnetic Resonance Imaging*; Wiley: Chichester, U.K., 2001.
(3) Werner, E. J.; Datta, A.; Jocher, C. J.; Raymond, K. N. *Angew. Chem., Int. Ed.* **2008**, *47*, 8568–8580.
(4) Jurisson, S.; Berning, D.; Jia, W.; Ma, D. *Chem. Rev. (Washington, DC, U.S.)* **1993**, *93*, 1137–1156.
(5) Reichert, D. E.; Lewis, J. S.; Anderson, C. J. *Coord. Chem. Rev.* **1999**, *184*, 3–66.

10.1021/ic900119a CCC: $40.75
Published on Web 03/12/2009

In recent years, ^{68}Ga has attracted a great deal of attention because of improvements in ^{68}Ge/^{68}Ga generator technology, providing ionic (non-complexed) $^{68}Ga^{3+}$ for an affordable price (for a recent review on ^{68}Ga-PET, see Fani et al.[6]). Moreover, ^{68}Ga can be regarded a particularly promising isotope for radioimaging purposes since some ^{68}Ga labeled peptides have recently been shown to exhibit distinctly better pharmacological properties than their ^{111}In labeled analogues[7−9] and ^{18}F based radiotracers.[10]

For imaging purposes, the radiometals have to be included into biomolecules (targeting vectors) which possess affinity to certain tissues, as, for example, in oncology to tumor cells. Unlike other PET radioisotopes such as ^{18}F or ^{11}C, ionic Ga^{3+} and In^{3+} can not be bound covalently to targeting vectors but must be complexed by a ligand which is conjugated to the vector. However, this has the advantage that labeling can be done just prior to the diagnostic exam, and loss of activity is thus kept to a minimum. Derivatives of polyazacycloalkanes bearing N substituents (pendant arms) with additional coordination sites have been found suitable for this purpose because of formation of very stable metal complexes. Depending on ring size and number of N atoms, a variety of chelators with different cavity sizes and denticities can be prepared on this basis. Among such compounds, derivatives of 1,4,7-triazacyclononane-1,4,7-triacetic acid (NOTA)[12] and particularly of 1,4,7,10-tetraazacyclododecane-1,4,7,10-tetraacetic acid (DOTA)[11] have been widely applied for metal complexation pertinent to medical imaging (see Scheme 1). These chelators also form stable complexes with both Ga^{3+} and In^{3+}[16,17] and can be bound to biomolecules as well. Ligands with other donors at the pendant arms have also been explored. Welch et al. prepared the amino-thiol-ligand 1,4,7-tris(mercaptoethyl)-1,4,7-triazacyclononane (TACN-TM, **L1**, see Scheme 2).[18] The crystal structures of both Ga**L1** and In**L1** complexes were determined;[18,19] thermodynamic stabilities[20] are exceeding by far the values found for complexes of these metals with NOTA and DOTA.[16,17]

Scheme 1. Known Azamacrocycle Based Chelating Agents[11−15]

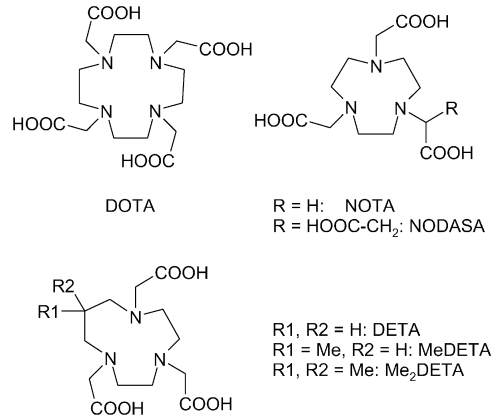

Scheme 2. Known (**L1**) and Novel (**L2**, **L3**) Ligands Studied in This Work

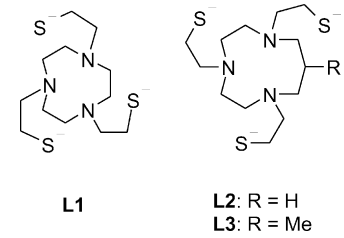

The Ga^{3+} ion is rather small (ion radius of hexacoordinate Ga^{3+} is 62 pm)[21] and therefore forms more stable complexes with ligands possessing small cavities, such as NOTA analogues. On the other hand, the larger In^{3+} (radius of hexacoordinate ion being 80 pm)[21] accordingly prefers ligands based on larger macrocycles, such as DOTA. In search for alternative synthetic routes toward bioconjugated chelators, the intermediate-sized azamacrocycle 1,4,7-triazacyclodecane ([10]aneN_3) has been used as ligand backbone in the past. Its triacetic acid derivative DETA[14] (see Scheme 1) was found to be suitable for both metals.[22] However, the 9-methylated analogues MeDETA and Me_2DETA were studied only with respect to complexation of Gd^{3+}.[15] More recently, Hovinen et al. reported an innovative route toward 9-substituted bioconjugated [10]aneN_3 derivatives but did not present a synthesis for the fully functional chelator including the necessary N-pendant sidearms.[23]

Compared to the plethora of information on complexes of NOTA and DOTA derivatives, the available data for complexes of DETA-like ligands is rather poor. In contrast to the first, no solid state structure of any metal complex for the latter has been published until now. Hence, a fundamental investigation of solid state and solution structures for complexes of both unsubstituted and backbone-functionalized

(6) Fani, M.; André, J. P.; Maecke, H. R. *Contrast Media Mol. Imaging* **2008**, *3*, 67–77.
(7) Antunes, P.; Ginj, M.; Zhang, H.; Waser, B.; Baum, R. P.; Reubi, J. C.; Maecke, H. *Eur. J. Nucl. Med. Mol. Imaging* **2007**, *34*, 982–993.
(8) Buchmann, I.; Henze, M.; Engelbrecht, S.; Eisenhut, M.; Runz, A.; Schäfer, M.; Schilling, T.; Haufe, S.; Herrmann, T.; Haberkorn, U. *Eur. J. Nucl. Med. Mol. Imaging* **2007**, *34*, 1617–1626.
(9) Gabriel, M.; Decristoforo, C.; Kendler, D.; Dobrozemsky, G.; Heute, D.; Uprimny, C.; Kovacs, P.; Von Guggenberg, E.; Bale, R.; Virgolini, I. J. *J. Nucl. Med.* **2007**, *48*, 508–518.
(10) Ambrosini, V.; Tomassetti, P.; Castellucci, P.; Campana, D.; Montini, G.; Rubello, D.; Nanni, C.; Rizzello, A.; Franchi, R.; Fanti, S. *Eur. J. Nucl. Med. Mol. Imaging* **2008**, *35*, 1431–1438.
(11) Stetter, H.; Frank, W. *Angew. Chem., Int. Ed. Engl.* **1976**, *88*, 760.
(12) Wieghardt, K.; Bossek, U.; Chaudhuri, P.; Herrmann, W.; Menke, B. C.; Weiss, J. *Inorg. Chem.* **1982**, *21*, 4308–4314.
(13) André, J. P.; Maecke, H. R.; Zehnder, M.; Macko, L.; Akyel, K. G. *Chem. Commun.* **1998**, 1301–1302.
(14) Takahashi, M.; Takamoto, S. *Bull. Chem. Soc. Jpn.* **1977**, *50*, 3413–3414.
(15) Brücher, E.; Cortes, S.; Chavez, F.; Sherry, A. D. *Inorg. Chem.* **1991**, *30*, 2092–2097.
(16) Clarke, E. T.; Martell, A. E. *Inorg. Chim. Acta* **1991**, *181*, 273–280.
(17) Clarke, E. T.; Martell, A. E. *Inorg. Chim. Acta* **1991**, *190*, 37–46.
(18) Moore, D. A.; Fanwick, P. E.; Welch, M. J. *Inorg. Chem.* **1990**, *29*, 672–676.
(19) Bossek, U.; Hanke, D.; Wieghardt, K.; Nuber, B. *Polyhedron* **1993**, *12*, 1–5.
(20) Ma, R.; Welch, M. J.; Reibenspies, J.; Martell, A. E. *Inorg. Chim. Acta* **1995**, *236*, 75–82.
(21) Shannon, R. D. *Acta Crystallogr., Sect. A: Found. Crystallogr.* **1976**, *32*, 751–767.
(22) Broan, C.; Cox, J. P.; Craig, A. S.; Kataky, R.; Parker, D.; Harrison, A.; Randall, A. M.; Ferguson, G. *J. Chem. Soc., Perkin Trans.* **1991**, *2*, 87–99.
(23) Hovinen, J.; Sillanpää, R. *Tetrahedron Lett.* **2005**, *46*, 4387–4389.

Scheme 3. Synthesis of Novel Ligands H_3**L2** and H_3**L3**[a]

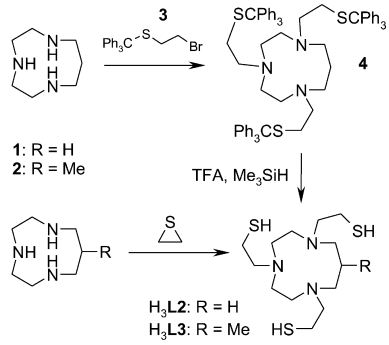

[a] The compounds were isolated as trihydrochlorides or, in case of cleavage of tritylthioethers, as tris(trifluoroacetate) salt.

pendant-arm triazacyclodecanes is still lacking. To assess the potential of such chelators, we synthesized two novel triazacyclodecane based thiol pendant arm ligands **L2** and **L3** in analogy to the mentioned [9]aneN_3 based compound **L1** (see Scheme 2). The metal complexes of **L3** can be regarded as structural models for the metal chelate subunit of possible bioconjugated radiopharmaceuticals. Particularly in comparison to triazacyclononane based ligands, we deem an assessment of cavity size and coordination geometry a very interesting issue. In addition, because of the asymmetry of the macrocycle and the presence of a methyl group substitution in the backbone of **L3**, a complicated structural chemistry is encountered; the insights gained herein can be generalized to similar ligands. The results of our investigation thus help to improve overall understanding of coordination behavior of pendant-arm azamacrocyclic ligands.

Results

Ligand and Complex Syntheses. The synthesis of the novel ligands is outlined in Scheme 3. We successfully applied the approach that Welch et al. employed for synthesis of **L1** (amine insertion into ethylene sulfide),[18] using [10]aneN_3 (**1**) and 9-methyl-[10]aneN_3 (**2**) as the amine components. As an alternative, we investigated N-alkylation using 2-(tritylmercapto)ethyl bromide (**3**), followed by cleavage of the S-trityl groups. However, this was only successful for the synthesis of **L2** because of badly reproducible and uneven alkylation of amine **2**.

Another problem was encountered for the insertion reaction of amines into ethylene sulfide. In this way, ligand **L3** was obtained contaminated with considerable amounts of byproduct that we were unable to remove. On the basis of MS spectra, the impurities were identified as thioether oligomers originating in nucleophilic attack of thiol moieties on ethylene sulfide. **L2** contained only minute amounts of such products, and not even traces were detected in case of **L1**. Apparently, in the latter case there is a good balance in the nucleophilicities of NH and SH moieties, which is disturbed by larger ring size and particularly by backbone substitution. Another reason for the observed change in reactivity could be the increased basicity of the 10-membered rings, presumably leading to partial deprotonation of thiols and thereby greatly increasing their nucleophilicity. As a conclusion, we like to point out that for other azamacrocycles, the results of the ethylene sulfide reaction are rather unpredictable; we therefore believe that it can not be considered a universal synthetic approach. However, despite of the impurities in **L3**, we were able to use it successfully for complex synthesis.

Fe^{3+} and Ga^{3+} complexes were obtained from methanolic solutions of ligand hydrochlorides, the appropriate metal salts, and an excess of diisopropylethylamine. The In^{3+} complexes were prepared in analogy to the procedure reported for In**L1**.[19] Anhydrous $InCl_3$ was dissolved in a solution of NaOMe in MeOH. Then the ligand was added, forming the desired complex. Crystals suitable for X-ray diffraction (XRD) were obtained by recrystallization from dimethylformamide (DMF) (Ga^{3+} and In^{3+} complexes) or taken directly from the reaction mixture (Fe^{3+} complexes). All complexes are insoluble in water and common solvents with the exception of DMF and dimethyl sulfoxide (DMSO) in which they are soluble to a small extent.

General Considerations Concerning Molecular Structures. Because of the asymmetry of the macrocycle [10]aneN_3, complexes of **L2** and **L3** can in principle adopt a plethora of conformers and stereoisomers. According to established nomenclature,[24−26] we will denote the overall helicity and the steric configuration of the chelate rings using the Scheme "c-H(rr)(sss)". The wildcard "c" can adopt the values "ch" (chair) and "tb" (twist-boat). It describes the conformation of the six-membered chelate ring involving the propylene or (2-methyl)propylene bridge. "H" is the overall helicity of the molecule (Δ or Λ). "r" and "s" describe the orientation of the ethylene in the five-membered chelate rings of the macrocycle and the pendant arms, respectively (each wildcard independently either δ or λ).

Regarding isomerism of molecular structures, complexes of **L2** and **L3** exhibit fundamental differences caused by the additional methyl group in **L3**. In uncomplexed **L3**, both the tertiary carbon and the ring nitrogens adjacent to the propylene bridge are prochiral and become stereocenters upon complexation. In the corresponding M**L3** complexes, the methyl group can be positioned either above (α) or below (β) the projection of the 6-membered ring, where below is defined as the same side as the N-atom not included in this ring (see also Scheme 4). Because of its steric demand, the α or β configuration forces the six-membered chelate ring to adopt the chair or twist-boat conformation, respectively. Since the sterical strain in the combinations α/tb and β/ch is so pronounced that they practically can be ruled out, the ch/tb notation hence also implicates a description of steric configuration of the tertiary carbon and the ring nitrogen atoms. Thus, we simplify the complete notations α-ch and β-tb to just ch and tb, respectively, similar to M**L2** complexes.

(24) Aime, S.; Botta, M.; Fasano, M.; Marques, M. P. M.; Geraldes, C. F. G. C.; Pubanz, D.; Merbach, A. E. *Inorg. Chem.* **1997**, *36*, 2059–2068.
(25) Corey, E. J.; Bailar, J. C. *J. Am. Chem. Soc.* **1959**, *81*, 2620–2629.
(26) Beattie, J. K. *Acc. Chem. Res.* **1971**, *4*, 253–259.

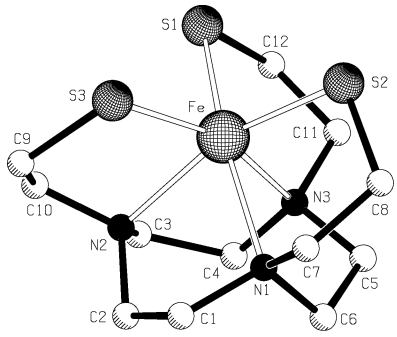

Fe**L1**

Figure 1. X-ray molecular structure of Fe**L1** (hydrogen atoms omitted for clarity).

The above furthermore implicates that for the M**L3** complexes the ch and tb forms are diastereomers, and ch ⇌ tb interconversion is actually a change of *configuration*. In contrast, for M**L2** these two forms exhibit the same bonding structure, and consequently ch and tb forms are merely different *conformations*. Hence it is appropriate to denote the ch/tb forms of M**L3** complexes as *diastereomers* and in case of M**L2** as *conformers*. Another conclusion is that for M**L3** complexes, the ch ⇌ tb interconversion requires cleavage of several coordination bonds, whereas this is not the case for M**L2**. The consequences resulting from this will be discussed below.

Crystal Structures. X-ray molecular structures for complexes of **L1**, **L2**, and **L3** are depicted in Figures 1, 2, and 3, respectively. To facilitate direct comparison of the structural data given in Table 1, the numbering of the heteroatoms is chosen in such way that S and N atoms with identical numbers are found at mutually opposite vertices of the trigonal-antiprismatic coordination sphere. For complexes of asymmetric ligands **L2** and **L3**, the numbering of the nitrogens corresponds to equivalent positions in the ligand framework.

Crystal lattices of all compounds are free of solvent molecules or additional ligands, and the coordination sphere generally involves all donors available. The complexes are thus uncharged. They form monomers with trigonal-antiprismatic *fac*-N_3S_3 coordination spheres, which exhibit varying degrees of distortion. Further, all compounds crystallized in non-chiral space groups and therefore as racemic mixtures of the chiral conformers. The structure of Fe**L1** unsurprisingly is very similar

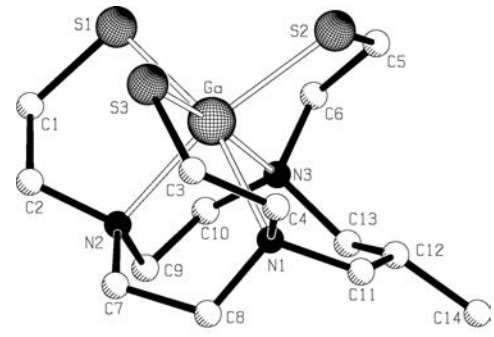

Ga**L3**

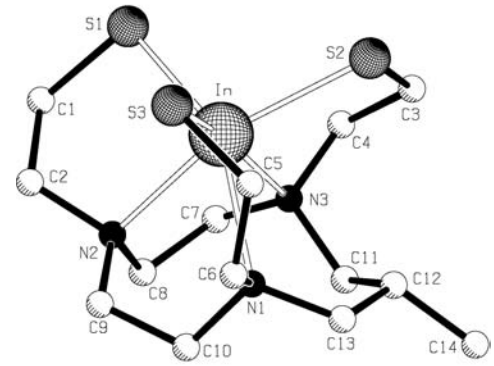

In**L3**

Figure 3. X-ray molecular structures of Ga**L3** and In**L3** (hydrogen atoms omitted for clarity). Note the inverse helicity of the C5–C6 pendant arm for In**L3**.

to its Ga^{3+} analogue,[18] exhibiting no particularities. All M**L2** complexes are present as ch-Δ(λλ)(δδδ)/ch-Λ(δδ)(λλλ) enantiomeric pair, whereas M**L3** compounds exhibit a different configuration in the solid state. The six-membered chelate rings adopt twist-boat configurations, Ga**L3** being present as tb-Δ(λλ)(δδδ)/tb-Λ(δδ)(λλλ) enantiomeric pair and In**L3** as tb-Δ(λλ)(λδδ)/tb-Λ(δδ)(δλλ), respectively.

Although the M−N bond distances of complexes of **L2** and **L3** are generally quite large in comparison to those of some **L1** analogues,[18,19,22] it seems worthwhile to point out that some complexes show single, extraordinarily long M−N coordination bonds. The Ga−N1 distances of Ga**L2** and Ga**L3** (2.324 Å) exceed by far the values of Ga**L1** (2.201 to 2.221 Å)[18] and [Ga(NOTA)] (2.046 to 2.078 Å).[22] The same applies for In**L3** (2.546 Å), as the In−N distances range from

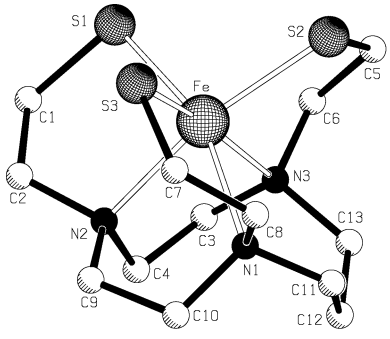

Fe**L2**

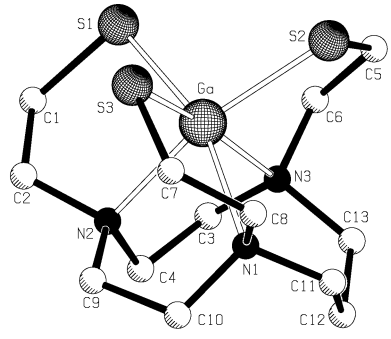

Ga**L2**

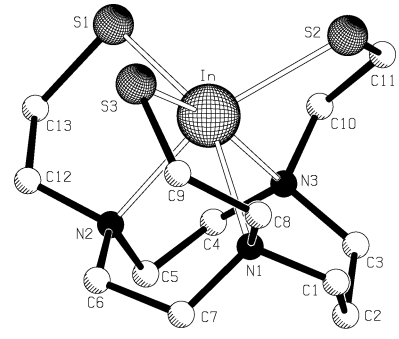

In**L2**

Figure 2. X-ray molecular structures of Fe**L2**, Ga**L2**, and In**L2** (hydrogen atoms omitted for clarity).

Table 1. Selected Bond Lengths [Å] and Angles [deg] for Compounds Fe**L1**, Fe**L2**, Ga**L2**, In**L2**, Ga**L3**, and In**L3**

	Fe**L1**	Fe**L2**	Ga**L2**	In**L2**	Ga**L3**	In**L3**
M−S1	2.3638(5)	2.3907(7)	2.4033(6)	2.543(1)	2.376(2)	2.5059(8)
M−S2	2.3393(5)	2.3236(7)	2.3191(6)	2.481(1)	2.328(2)	2.5294(8)
M−S3	2.3576(5)	2.3398(7)	2.3404(6)	2.490(1)	2.338(2)	2.4836(8)
M−N1	2.268(2)	2.331(2)	2.324(2)	2.449(3)	2.324(4)	2.546(2)
M−N2	2.241(2)	2.235(2)	2.191(2)	2.360(3)	2.190(4)	2.407(2)
M−N3	2.262(2)	2.294(2)	2.271(2)	2.416(3)	2.230(4)	2.369(2)
∠S1−M−N1	159.06(4)	159.77(6)	161.68(4)	155.30(8)	163.6(1)	153.66(6)
∠S2−M−N2	161.72(4)	162.75(6)	163.41(5)	156.68(8)	163.8(1)	155.31(6)
∠S3−M−N3	161.07(4)	170.16(5)	171.02(4)	164.79(8)	171.9(1)	162.58(6)
∠N1−M−N2	77.80(6)	76.94(7)	77.64(6)	74.1(1)	79.0(2)	73.62(8)
∠N1−M−N3	76.81(5)	86.95(7)	87.37(6)	84.2(1)	87.3(2)	83.83(8)
∠N2−M−N3	77.76(5)	80.81(7)	81.23(6)	77.4(1)	80.4(2)	74.96(8)

Table 2. Calculated (B3LYP) Bond Distances [Å] of the Metal Coordination Environments for M**L2** and M**L3** Complexes (M = Ga^{3+}, In^{3+})

	Ga**L2** ch-Δ(λλ)(δδδ)		Ga**L3** tb-Δ(λλ)(δδδ)		In**L2** ch-Δ(λλ)(δδλ)		In**L3** tb-Δ(λλ)(δδδ)	
	vacuo	DMSO	vacuo	DMSO	vacuo	DMSO	vacuo	DMSO
M−S1	2.379	2.446	2.371	2.420	2.522	2.565	2.505	2.550
M−S2	2.337	2.377	2.352	2.218	2.478	2.514	2.498	2.537
M−S3	2.354	2.399	2.340	2.258	2.494	2.528	2.467	2.505
M−N1	2.498	2.340	2.368	2.420	2.562	2.455	2.756	2.555
M−N2	2.290	2.296	2.308	2.218	2.432	2.357	2.494	2.408
M−N3	2.426	2.220	2.614	2.258	2.523	2.409	2.467	2.384

2.379 to 2.408 Å for In**L1**[19] and from 2.288 to 2.331 for [In(NOTA)·HCl·H_2O].[22] In addition, large differences in M−S and particularly in M−N bond lengths within one molecule can be observed for the mentioned complexes. For both Ga**L2** and Ga**L3**, the longest and shortest Ga−N distances differ by 0.13 Å, and for In**L3** by 0.17 Å.

Density Functional Theory (DFT) Calculations. Aiming to obtain information about the solution structure of the Ga^{3+} and In^{3+} complexes of **L2** and **L3**, these systems were characterized by means of DFT calculations. Structure optimizations of the Ga^{3+} and In^{3+} complexes of **L2** and **L3** were first carried out for the respective structures that were observed in the solid state. The calculated bond distances of the metal coordination environments are given in Table 2. In addition, we performed structure optimizations modeling solvent influences with the IEF-PCM model, applying parameters of DMSO because this solvent was used for NMR measurements. This resulted in slightly increased M−S distances and a dramatic shortening of most of the M−N bonds in comparison to the structures optimized in vacuo. The latter effect is particularly pronounced for Ga^{3+} complexes (up to 0.36 Å) but less important for In^{3+} compounds (<0.2 Å). However, it is not surprising that in vacuo calculations clearly overestimate the M−N bond distances, as a dramatic shortening of M−N bonds upon inclusion of solvent effects has been previously observed for different metal complexes with ligands based on aza- and oxaazamacrocycles.[27−29] The geometries obtained including solvent modeling show good agreement with X-ray structures, differences between calculated and measured bond lengths being less than 0.05 Å for In^{3+} and 0.11 Å for Ga^{3+} complexes, respectively.

To disclose possible solution structures of M**L2** and M**L3** (M = Ga^{3+}, In^{3+}), we performed conformational analyses for these systems. As a first step, we considered those conformations that show identical configuration for the three five-membered chelate rings formed upon coordination of the pendant arms, as well as for the two five-membered chelate rings formed upon coordination of the ethylenediamine moieties. Of the resulting enantiomeric pairs, only one enantiomer was considered. Hence, the tb-Λ(λλ)(λλλ), ch-Λ(λλ)(λλλ), tb-Δ(λλ)(δδδ), and ch-Δ(λλ)(δδδ) geometries were calculated, including solvent effects as mentioned above. Cartesian coordinates, as well as tables of bond distances and angles of the coordination environments, are provided as Supporting Information. Relative Gibb's free energies for the calculated isomers are given in Figure 4. The calculations show that the ch-Δ(λλ)(δδδ) form is likely to be the most stable isomer for all complexes. In comparison, the tb-Δ(λλ)(δδδ) forms are predicted to be considerably destabilized by Δ*G* values ranging from 8.8 to 13.1 kJ mol^{-1}; this effect is less pronounced for the In^{3+} complexes. Inversion of the helicity of only the (N−M−N) containing five-membered chelate rings accounts for another Δ*G* increase in all cases; hence it can be assumed that the Λ(λλ)/Δ(δδ) conformers generally play no role.

NMR Investigation. Two distinct sets of resonances can be found in the ^{13}C NMR spectra of all complexes: a group with chemical shifts between 18 and 28 ppm and another one at 45−69 ppm. On the basis of simulations,[30] the first set of resonances can be assigned the three methylene groups adjacent to the sulfur atoms and the methyl carbon (the latter only for M**L3** complexes). For the signals between 45−69 ppm an unambiguous assignment was impossible. ^1H NMR spectra of all compounds are very crowded and show line broadening due to exchange phenomena. We focused our attention on the signals of the middle methylene group of

(27) Cosentino, U.; Villa, A.; Pitea, D.; Moro, G.; Barone, V.; Maiocchi, A. *J. Am. Chem. Soc.* **2002**, *124*, 4901–4909.
(28) Platas-Iglesias, C.; Mato-Iglesias, M.; Djanashvili, K.; Muller, R. N.; Vander Elst, L.; Peters, J. A.; de Blas, A.; Rodríguez-Blas, T. *Chem.—Eur. J.* **2004**, *10*, 3579–3590.
(29) Platas-Iglesias, C.; Esteban, D.; Ojea, V.; Avecilla, F.; deBlas, A.; Rodríguez-Blas, T. *Inorg. Chem.* **2003**, *42*, 4299–4307.
(30) *ACD NMR prediction software*, Version 3.00; Advanced Chemistry Development, Inc.: Toronto, Canada; http://www.acdlabs.com (accessed Jan 15, 2009).

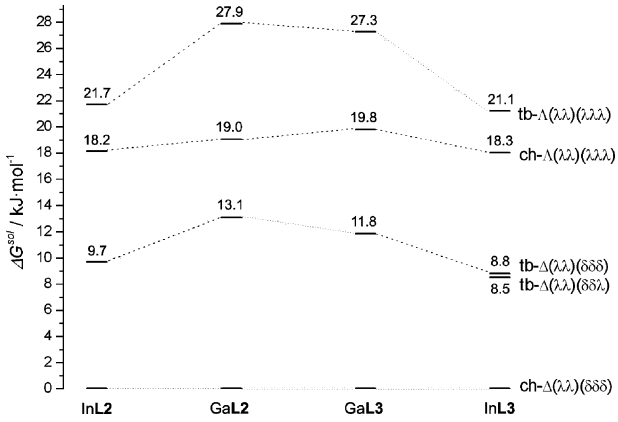

Figure 4. Relative free energies ΔG [kJ mol^{-1}] of different conformers and diastereomers of M**L2** and M**L3** complexes (M = Ga^{3+}, In^{3+}) obtained from DFT calculations including solvent modeling. For each individual compound, ΔG^{sol} of the ch-$\Delta(\lambda\lambda)(\delta\delta\delta)$ form is set to zero and all other values are relative to it.

the propylene bridge (M**L2** complexes) and the methyl signals (M**L3** complexes), which can be evaluated because these resonances are isolated from the rest of the spectra as a result of their relatively low chemical shifts.

GaL2. At room temperature, the ^{13}C NMR spectrum of Ga**L2** shows four resonances in the range of 23−26 ppm and another nine between 45−63 ppm. The total of 13 signals complies with a solution structure similar to the one found in the solid state. Upon increase of the temperature, the resonances at 24.4 and 24.5 ppm coalesce at about 50 °C, whereas the other resonances severely broaden until at 85 °C only three signals could be discerned. From the coalescence temperature of two sets of coalescing resonances, the barrier for interconversion was estimated to be $\Delta G^{\#} = 70 \pm 3$ kJ mol^{-1}. Barriers of similar magnitude were observed for interconversions between $\Delta(\delta\delta\delta\delta)$ and $\Lambda(\lambda\lambda\lambda\lambda)$ forms of Yb^{3+}-DOTA complexes.[31] Hence we assume that at room temperature, Ga**L2** indeed adopts the structure known from solid state, being present as racemic mixture of interconverting ch-$\Delta(\lambda\lambda)(\delta\delta\delta)$ and ch-$\Lambda(\delta\delta)(\lambda\lambda\lambda)$ enantiomers.

InL2. In contrast to Ga**L2**, the ^{13}C NMR spectrum of In**L2** at room temperature shows only eight signals, some of which were broadened. Upon increase of the temperature these signals sharpened, suggesting that a coalescence occurs somewhat below room temperature. Apparently, In**L2** also exhibits a solution structure similar to the one found in the solid state, the difference being that exchange between enantiomers is much faster than for Ga**L2**. Given that the chemical shift differences for Ga**L2** and for In**L2** are approximately the same and the coalescence temperature is between 0 and 25 °C, the Gibb's free energy barrier of interconversion can be estimated to be $\Delta G^{\#} = 50-65$ kJ mol^{-1}.

GaL3. At room temperature, the ^{13}C NMR spectrum of Ga**L3** shows 26 resonances, 8 in the range 18−28 ppm and 18 between 46 and 68 ppm. Only single ^{13}C resonances were observed for the tertiary carbon and the CH_3 group. Upon increase of the temperature, the signals at 25.8 and 25.7 ppm coalesce to a single resonance at 25 ppm. From this coalescence, the interconversion barrier was estimated to be $\Delta G^{\#} = 70 \pm 3$ kJ mol^{-1}, a value similar to that for Ga**L2**. No further dynamic phenomena were observed for the other signals in the range 18−28 ppm. However, severe line broadening occurred in most of the resonances in the range 46−68 ppm. At 85 °C, only three signals could be discerned. Our interpretation is that the chair and twist-boat diastereomers of this complex are both present in the solution. As stated above, their interconversion would require considerable energy because of partial decoordination of the ligand; thus, it occurs slow on the NMR time scale. The observed coalescence is rooted in interconversion of the two enantiomers, $\Delta(\lambda\lambda)(\delta\delta\delta)$ and $\Lambda(\delta\delta)(\lambda\lambda\lambda)$, for both ch and tb diastereomers. In contrast to ^{13}C NMR, only little information can be discerned from the ^{1}H NMR spectrum of Ga**L3**, as it is very complicated. However, two major doublets are observed for the methyl group which we assume to be associated to the most stable conformers of the ch and tb forms, thus corroborating the interpretation of the ^{13}C NMR spectra. In addition, several doublet signals of small intensity are present, which presumably correspond to some less stable conformers, for example, conformers with different orientations of the CH_2CH_2S pendant arms.

InL3. The spectrum of the In**L3** complex, once again, is simpler. Only four resonances were observed at 18−30 ppm and another four at 51−64 ppm. The resonances at 51.1 and 61.9 ppm were broadened at room temperature but sharpened at higher temperatures. From the low number of resonances it can be concluded that this complex occurs only as a single enantiomeric pair with rapid exchange on the ^{13}C NMR time scale between the enantiomers. An unambiguous assignment to either the chair or the twist-boat isomer is impossible on the basis of these data.

Asesssment of Solution Structures from ^{1}H NMR Data. From ^{13}C NMR spectra it is not possible to disclose the actual conformation of the six-membered chelate rings. Hence, vicinal proton−proton coupling constants of the propylene hydrogens were calculated from the H2−C2−C3−H3 and H4−C4−C3−H3 dihedrals of the DFT calculated ch-$\Delta(\lambda\lambda)(\delta\delta\delta)$ and tb-$\Delta(\lambda\lambda)(\delta\delta\delta)$ structures of Ga**L2**, In**L2**, Ga**L3**, and In**L3** and compared to experimental values (see also Experimental Section). For the calculations the program Mspin[32] was employed which is based on the empirically generalized Karplus[33]type equation of Haasnoot, de Leeuw, and Altona.[34] A comparison of the values thus obtained with experimental data is given in Table 3 (for atom numbering see Scheme 4). For Ga**L3**, experimental determination of coupling constants was not possible because of the crowded spectra; for the sake of completeness, the calculated values are nonetheless given.

Values for axial-axial coupling constants for chair conformations are usually >12 Hz, whereas for boat conforma-

(31) Jacques, V.; Desreux, J. F. *Inorg. Chem.* **1994**, *33*, 4048–4053.
(32) Navarro, A. *Mspin*, 1.0.0; Mestrelab research SL: Santiago de Compostela, 2008; http://www.mestrec.com (accessed Jan 15, 2009).
(33) Karplus, M. *J. Am. Chem. Soc.* **1963**, *85*, 2870–2871.
(34) Haasnoot, C. A. G.; de Leeuw, F. A. A. M.; Altona, C. *Tetrahedron* **1980**, *36*, 2783–2792.

Table 3. Experimental and Calculated[32] Absolute Values of Vicinal Proton−Proton Coupling Constants [Hz] in the Six-Membered Chelate Rings of Ga**L2**, In**L2**, Ga**L3**, and In**L3**[a]

	Ga**L2**			In**L2**			Ga**L3**		In**L3**		
$^3J_{HH}$	exp	ch	tb	exp	ch	tb	ch	tb	exp	ch	tb
(2/4)α3α	3.3−3.8	2.0	3.7	2.6	1.9	3.2		3.3	3.2[c]		2.9
(2/4)α3β	12.8	12.5	3.7	12.8	12.5	4.3	11.7		10.6[b]	11.7	
(2/4)β3α	3.3−3.8	4.1	11.5	4.3	4.3	11.7		11.1	10.6[c]		11.1
(2/4)β3β	2.8	2.9	3.2	2.5	2.8	2.6	2.8		3.2[b]	2.3	

[a] The experimental error is ± 0.1 Hz. Calculated values for equivalent $^3J_{H2H3}$ and $^3J_{H3H4}$ coupling constants were averaged. [b] Assignment valid only for ch diastereomer (methyl group in α position). [c] Assignment valid only for tb diastereomer (methyl group in β position).

Scheme 4. Labelling of Nuclei Used in Table 3

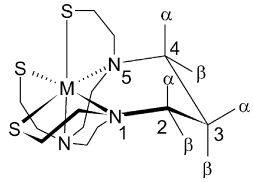

tions generally 10−11 Hz are found.[34] Hence the coupling constants may provide information on possible conformations of the six-membered ring. The fact that for each complex one of the experimentally determined coupling constants is larger than 10.6 Hz is a strong proof that for the three complexes investigated there are no fast ch ⇌ tb equilibria with substantial contributions of each of the conformations. The latter would have resulted in considerably smaller values for the coupling constant concerned.

The data comparison in Table 3 shows that the fit of experimental and calculated values is quite good for Ga**L2** and In**L2**. The values of experimental (12.8 Hz) and calculated (12.5 Hz) axial-axial coupling constants indicates that these complexes indeed adopt the ch conformation in solution. However, for In**L3** the calculated values for both ch and tb diastereomers are more or less in accord with the experiment, although the match is slightly closer for the tb isomer and the experimental axial-axial coupling of 10.6 Hz is typical for boat conformers. We thus hold the view that these data can not unambiguously prove the presence of either isomer.

Discussion

Structure in Solution. According to computational results, all complexes would be expected to exhibit the six-membered chelate ring in the chair conformation as DFT calculations predict it to be considerably more stable in DMSO solution. In regard to M**L2** complexes there is little doubt to this, since all experimental results support the view that indeed the predicted conformation with exchanging enantiomers ch-Λ($\delta\delta$)($\lambda\lambda\lambda$) and ch-Δ($\lambda\lambda$)($\delta\delta\delta$) is adopted. This result readily comes up to our expectations, as in a previous NMR study of DETA complexes with various metals it has been found that the six-membered chelate ring always adopts the chair conformation.[35] The results of XRD are consistent with this picture.

As stated above, a different situation is encountered for M**L3**. Unlike for M**L2** compounds, ch ⇌ tb interconversion of M**L3** complexes is a change of configuration and requires intermediate cleavage of several coordination bonds. It should be borne in mind that the starting material used for preparation of solutions for NMR measurements has been the twist-boat diastereomer, as is evident from XRD studies. If the chair diastereomer is observed in solution this implies that tb → ch interconversion and thus partial dissociation actually takes place upon dissolving the solid samples; this appears even more probable as in all cases dissolution of the solid material prior to NMR measurement required heating to 60−70 °C.

As we know from ^{13}C NMR, in case of Ga**L3** a mixture of ch and tb forms is present in solution. For In**L3**, determination of the solution structure is not unambiguously possible by experimental means, as assessment from coupling constants does not allow for a definite decision. However, coordination environments of the In^{3+} complexes generally seem to be less rigid. This is apparent from the observation that in contrast to Ga^{3+} complexes, their ^{13}C NMR spectra exhibit fewer signals because of low coalescence temperatures for the interconversion equilibrium of enantiomers. As configurational exchange, although very slowly, occurs for Ga**L3**, we suppose that this is also the case for In**L3**, yet again considerably faster than for the Ga^{3+} complex. This view is supported by earlier studies on metal complexes of the related ligand DETA[22,35] (see Scheme 1). In an NMR study performed by Geraldes et al.,[35] these authors state that large ions, namely, Ba^{2+} and In^{3+}, bind considerably weaker to the ring nitrogens than Ga^{3+}, which is reflected in broader NMR peaks and facilitated dissociation of the complexes. Hence, we assume that the single diastereomer observed in In**L3** solutions is most probably the ch form, in accordance with the computational results, although no real evidence can be provided for this view.

Ring Size and Substitution Effects. Another goal of this study was to compare the well-known complexation behavior of pendant-arm triazacyclononanes with that of equivalent triazacyclodecanes, particularly emphasizing changes of bond distances and geometry. Hence we also consider X-ray structural data of the Ga^{3+} and In^{3+} complexes of **L1**.[18,19] For the sake of facile comparison of structures, a summary of average M−S and M−N bond distances as well as average S−M−N bond angles for all known complexes of **L1**, **L2**, and **L3** is given in Table 4.

The change from **L1** to **L2** generally effects larger S−M−N angles. However, bond length alteration shows differences between the metals. For the iron complexes, the average Fe−N bond distances are increased by +0.02 Å, whereas Fe−S bonds remain unchanged. Compared to Ga**L1**,

(35) Geraldes, C. F. G. C.; Marques, M. P. M.; Sherry, A. D. *Inorg. Chim. Acta* **1998**, *273*, 288–298.

Table 4. Average Values for M−S and M−N Bond Distances [Å] and S−M−N Angles [deg] of Metal Complexes of Ligands **L1**-**L3**[a]

Metal	Ligand	∅ M−S	∅ M−N	∅ ∠S−M−N
Fe^{3+}	**L1**	2.35	2.26	160.6
	L2	2.35	2.28	164.2
Ga^{3+}	**L1**[18]	2.34	2.21	164.0
	L2	2.35	2.26	165.4
	L3	2.35	2.25	166.4
In^{3+}	**L1**[19]	2.51	2.40	155.0
	L2	2.50	2.41	158.9
	L3	2.51	2.44	157.2

[a] Additional structural data for Ga**L1**[18] and In**L1**[19] was taken from the literature.

Ga**L2** exhibits a slight (+0.01 Å) elongation of Ga−S bonds, but a large (+0.05 Å) elongation for the Ga−N linkages. In contrast, In**L2** shows just slightly (+0.01 Å) longer In−N bonds and even shorter (− 0.01 Å) In−S bonds than its **L1**-based equivalent. Hence, it can be concluded that the cavity of **L2** is slightly too large for optimal hosting of Ga^{3+} and Fe^{3+}. For In^{3+}, **L2** is more appropriate than **L1**, particularly with respect to the smaller degree of deformation of the octahedral coordination environment, as indicated by increased (+3.9°) S−In−N angles.

The methyl substitution of M**L3** complexes again effects marked differences to the M**L2** equivalents. For the Ga^{3+} compounds, unchanged Ga−S and slightly decreased (−0.01 Å) Ga−N bonds, as well as increased (+1.0°) S−Ga−N angles, are found. The opposite situation is found for the In^{3+} complexes, where increased In−S (+0.01 Å) and In−N (+0.03 Å) linkages and decreased average S−In−N (− 1.7°) angles are observed. Apparently, methyl substitution stabilizes the structure of Ga**L3** in comparison to Ga**L2**, whereas the structure of In**L3** is disadvantageous compared to In**L2**.

The question remains why in solid state the tb configuration for M**L3** complexes is chosen by nature. Calculations have unambiguously shown that this isomer is less stable in DMSO. However, as an exchange between configurations is possible in solution, the isomer finally precipitating is either less soluble in the solvent from which the complex was precipitated (DMF), or the crystal possesses a larger free enthalpy of the crystal lattice. The minor issue of why In**L3** in solid state adopts a rather unusual combination of pendant-arm helicities, ($\lambda\delta\delta$) and ($\delta\lambda\lambda$), can probably be regarded just an accidental freak of nature as the calculated ΔG of ($\lambda\delta\delta$) and ($\delta\delta\delta$) forms are identical within the accuracy limits of computation (see Figure 4).

Conclusions

Despite the fact that the cavity of **L3** is apparently not ideally suited for both Ga^{3+} and In^{3+}, this type of ligand can still be considered appropriate for complexation of both metals. Hence, we conclude that backbone-functionalized pendant-arm triazacyclodecanes are generally suitable for a wide range of small and medium sized metal ions. Radiopharmaceuticals based on such chelators therefore could be particularly suitable for the use with multiple radioisotopes and therefore applicable for a variety of purposes. We thus propose a high potential of this kind of ligands for applications in nuclear imaging.

Experimental Section

General Procedures. All reagents used were of analytical purity. Solvents were dried according to common methods. Ethylene sulfide and dry HCl gas were obtained from Aldrich and used without further treatment. NMR spectra of all compounds but the metal complexes were recorded using a Bruker AC 250 or a Bruker AC 400 spectrometer at 300 K. IR data was collected from the neat substances using a Nicolet Avatar 320 FT-IR spectrometer. Elemental analysis was performed using a Heraeus Vario EL III system. Melting points were determined with a Büchi Melting Point B 545 apparatus and are uncorrected. Mass spectra were recorded using a Finnigan MAT SSQ 710 and a Finnigan MAT 900XL TRAP, respectively.

Starting Materials. Ligand **L1**[18] and 1,3-di(p-toluolsulfonyloxy)-2-methylpropane[36] were prepared according to literature methods. The preparation of 1,4,7-triazacyclodecane (**1**, [10]aneN_3, TACD) followed essentially a published procedure,[37] with alterations as described before.[38]

9-Methyl-1,4,7-triazacyclodecane (Me[10]aneN_3, MeTACD) (2). This compound has been prepared before by Brücher et al., although using another reaction pathway.[15] A solution of 1,4,7-tri(p-toluolsulfonyl)-1,4,7-triazaheptane disodium salt (90 mmol, 55 g) and 1,3-di(p-toluolsulfonyloxy)-2-methylpropan (36 g, 90 mmol) in DMF (2 L) was heated to 120 °C for 3 h. The solution was concentrated to 500 mL and poured onto ice water (2 L). The white solid was filtered off and dried in vacuo. Purification was done by refluxing in ethanol (1 L) for 3 h and warm filtration. Obtained were 28 g (70%) of pure 9-methyl-1,4,7-tri(p-toluolsulfonyl)-1,4,7-triazacyclodecane. ^{1}H NMR (250 MHz, $CDCl_3$): δ = 0.86 [d, 3H, J = 7.1Hz], 2.42 [s, 9H], 2.81 [m, 4H], 3.19 [m, 2H], 3.41 [m, 4H], 3.79 [m, 2H], 7.32 [d, 6H, J = 8.0Hz], 7.71 [d, 6H, J = 8.2Hz] ppm. ^{13}C NMR (62.9 MHz, $CDCl_3$): 18.2, 21.5, 35.6, 52.0, 52.9, 57.1, 127.5, 127.7, 129.8 [2C], 134.3, 135.2, 143.7, 143.9 ppm.

The trisulfonamide was dissolved in 96% sulfuric acid and heated to 110 °C for 3 days. Then the mixture was added carefully with cooling and stirring to an excess of saturated aqueous sodium hydroxide solution and left standing overnight to complete crystallization of sodium sulfate. The inorganic salts were filtered off and washed thoroughly with chloroform. The remaining aqueous solution was extracted with chloroform (5 × 100 mL), all chloroform extracts were dried over anhydrous sodium sulfate and then the solvent was removed in vacuo. The oily residue was purified by kugelrohr distillation to yield the free amine as a colorless oil (3.75 g, 66%). ^{1}H NMR (250 MHz, $CDCl_3$): 2.33 [d, 3H, J = 6.9Hz], 3.42−3.77 [m, 1H], 3.81−4.78 [m, 13H], 9.35 [2H] ppm. ^{13}C NMR (62.9 MHz, $CDCl_3$): 19.2, 33.1, 48.5, 50.5, 58.0 ppm.

2-Bromoethyl Trityl Sulfide (3). Literature syntheses of this compound have been performed starting from lithiated dibromoethane.[39] However, we successfully applied an elegant method known from the synthesis of the corresponding chloro compound[40] which also produces excellent yields for **3**. To a solution of triphenylmethylbromide (11.3 g, 35 mmol) in dichloromethane (80

(36) Nelson, E. R.; Maienthal, M.; Lane, L. A.; Benderly, A. A. *J. Am. Chem. Soc.* **1957**, *79*, 3467–3469.
(37) Richman, J. E.; Atkins, T. J. *J. Am. Chem. Soc.* **1974**, *96*, 2268–2270.
(38) Notni, J.; Görls, H.; Anders, E. *Eur. J. Inorg. Chem.* **2006**, *144*, 4–1455.
(39) Meegalla, S.; Ploessl, K.; Kung, M.-P.; Stevenson, D. A.; Liable-Sands, L. M.; Rheingold, A. L.; Kung, H. F. *J. Am. Chem. Soc.* **1995**, *117*, 11037–11038.
(40) Trujillo, D. A.; McMahon, W. A., Jr.; Lyle, R. E. *J. Org. Chem.* **1987**, *52*, 2932–2933.

mL) was added ethylene sulfide (4.2 g, 70 mmol), and the mixture stirred overnight at r.t. Then the solvent was evaporated to dryness to remove the excess of ethylene sulfide, whereupon an off-white solid precipitated. It was redissolved in dichloromethane (30 mL), and upon addition of ethanol (50 mL) a precipitate was formed immediately. The solution was left standing for 1 h to complete crystallization. The product was filtered off, washed with ethanol, and dried in vacuo to give colorless crystals, mp 137 °C, in 94% yield (based on triphenylmethylbromide). ^{1}H NMR (250 MHz, $CDCl_3$): δ = 2.70−2.92 [m, 4H, (CH_2)$_2$], 7.14−7.47 [m, 15H, C_6H_5] ppm. ^{13}C NMR (62.9 MHz, $CDCl_3$): 30.0, 34.2, 67.5, 126.9, 128.3, 129.5, 144.5 ppm. Anal. Calcd for $C_{21}H_{19}SBr$ (383.35): C, 65.80; H, 5.00; S, 8.36; Br, 20.84. Found C, 65.75; H, 4.99; S, 8.20; Br, 21.16.

Ligand and Complex Syntheses. 1,4,7-Tris(2-trityl-mercaptoethyl)-1,4,7-triazacyclodecane (4). A solution of **3** (10 mmol, 3.8 g), [10]aneN_3 (**1**, 2 mmol, 286 mg), K_2CO_3 (10 mmol, 1.4 g), and NaI (10 mmol, 1.5 g) in dioxane (50 mL) was refluxed for 5 h. After cooling, the mixture was filtered, the solvent evaporated, and the residue subjected to chromatography on silica gel (eluent: $CHCl_3$ with 5% MeOH). The fractions containing the product were collected, and the solvent was removed in vacuo. Then a small amount dichloromethane was added, and by sudden exposure to vacuum the substance was obtained as a foam which could be dried easily to obtain the title compound as a white amorphous powder containing 2 molar equivalents of dichloromethane. ^{1}H NMR (250 MHz, $CDCl_3$): 2.24−3.21 [m, C**H**$_2$, ≈ 26H], 7.16−7.42 [m, Ar-**H**, ≈ 45H] ppm. ^{13}C NMR (62.9 MHz, $CDCl_3$): 20.2, 25.4, 28.8, 49.4, 52.2, 52.5, 52.7, 67.1, 67.7, 126.9, 127.1, 128.1, 128.2, 129.5, 144.1, 144.5 ppm. MS (FAB): 1050 (M+H). Anal. Calcd for $C_{70}H_{71}N_3S_3 \cdot 2\ CH_2Cl_2$ (1135.49): C, 70.86; H, 6.19; N, 3.44; S, 7.88, Cl, 11.62. Found C, 70.50; H, 6.09; N, 3.42; S, 8.10, Cl, 11.30.

1,4,7-Tris(mercaptoethyl)-1,4,7-triazacyclodecane Trihydrochloride (H_3L2·3 HCl). To a solution of [10]aneN_3 (7 mmol, 1.0 g) in dry toluene (50 mL) was added ethylene sulfide (41 mmol, 2.5 g, 2.5 mL), and the mixture heated to 50 °C for 3.5 h. Then the solvent was evaporated in vacuo, and the residue dissolved in dry diethyl ether (150 mL). The solution was filtered, cooled to − 20 °C, and a saturated solution of HCl gas in dry ether was added dropwise with stirring, whereupon a colorless, fine-crystalline precipitate was formed. After standing for several minutes to complete precipitation, the product was filtered off, washed with excess diethyl ether, and dried in vacuo to give 2.8 g of the title compound as a colorless hygroscopic solid. For repeated reactions, yields ranging from 72−92%, based on [10]aneN_3, were obtained. ^{1}H NMR (250 MHz, D_2O): δ = 2.29 [s, broad, 2H], 2.66−2.70 [m, 2H], 2.83 [t, 6H, J = 14.8], 3.05 [s, broad, 4H], about 3.3−3.7 [m, broad, 12H] ppm. ^{13}C NMR (62.9 MHz, D_2O): 18.2, 19.5, 48.0 (broad), 50.3 (broad), 58.4 (v. broad) ppm. Anal. Calcd for $C_{13}H_{32}N_3S_3Cl_3$ (432.98): C, 36.06; H, 7.45; N, 9.70; S, 22.22, Cl, 24.56. Found C, 36.28; H, 7.19; N, 9.81; S, 22.30; Cl, 24.10.

1,4,7-Tris(mercaptoethyl)-1,4,7-triazacyclodecane Tris(trifluoroacetate) (H_3L2·3 TFA). Trifluoroacetic acid (5 mL) was added to **4** (620 mg, 0.6 mmol) whereupon an orange colored slurry was obtained. Triethylsilane (0.37 mL, 2.3 mmol) was added at 0 °C, and the mixture was stirred for 30 min. Then it was allowed to warm to r.t., and water (20 mL) was added. The mixture was extracted three times with hexane and evaporated to dryness to give 300 mg (75% of theory) of a viscous oil which, upon prolonged drying in vacuo, turned into a white, amorphous solid. NMR spectra in D_2O were practically identical to those obtained for H_3**L2**·3 HCl, with additional signals from trifluoroacetate: ^{13}C NMR (62.9 MHz, D_2O): 116.2 [q, **C**F_3, J = 288.4Hz], 162.7 [q, **C**(O)O$^-$, J = 35.7Hz] ppm.

1,4,7-Tris(mercaptoethyl)-1,4,7-triazacyclononyliron(III) (FeL1). H_3**L1**·3 HCl (0.5 mmol, 210 mg) was dissolved in anhydrous MeOH (20 mL), a few drops of diisopropylethylamine were added, and the mixture was heated to 60 °C. Then a solution of Fe(acac)$_3$ (0.5 mmol, 177 mg) in MeOH (5 mL) was added quickly, whereupon the color of the solution changed to deep purple and a slow crystallization commenced. After 3 h the precipitate was filtered off, washed with EtOH and diethyl ether, and dried in vacuo to yield 95 mg (62%) of violet crystals. MS (DEI): m/z = 362 (M·$^+$). Anal. Calcd for $C_{12}H_{24}N_3S_3Fe$ (362.39): C, 39.77; H, 6.68; N, 11.60; S, 26.55. Found C, 39.80; H, 6.70; N, 11.80; S, 27.90.

1,4,7-Tris(mercaptoethyl)-1,4,7-triazacyclodecylgallium(III) (GaL2). H_3**L2**·3 HCl (0.5 mmol, 216 mg) was dissolved in anhydrous MeOH (10 mL), a few drops of diisopropylethylamine were added, and the mixture was heated to 60 °C. Then a solution of $Ga(NO_3)_3 \cdot 9\ H_2O$ in 10 mL of anhydrous MeOH was added dropwise. A white precipitate was obtained immediately, which was filtered off, washed with ethanol and ether, and dried in vacuo. Recrystallization from 7 mL of dry DMF yielded 73 mg (37%) of the title compound as small colorless prisms. ESI-MS (MeOH): m/z = 390, 392 (M+H). Anal. Calcd for $C_{13}H_{26}N_3S_3Ga$ (390.29): C, 40.01; H, 6.49; N, 10.77; S, 24.65. Found C, 40.01; H, 6.49; N, 10.85; S, 25.00.

1,4,7-Tris(mercaptoethyl)-1,4,7-triazacyclodecylindium(III) (InL2). Sodium (ca. 0.1 g) was dissolved in absolute ethanol. Then anhydrous $InCl_3$ (0.5 mmol, 110 mg) was added, and the mixture stirred until a clear solution was obtained. Solid H_3**L2**·3 HCl (0.5 mmol, 216 mg) was added, whereupon a white precipitate was obtained. The mixture was stirred for additional 3 h at 50 °C. Then the precipitate was filtered off, washed with MeOH and dried. Recrystallization from 20 mL of dry DMF yielded 90 mg (41%) of the title compound as small colorless prisms. ESI-MS (MeOH): m/z = 436 (M+H). Anal. Calcd for $C_{13}H_{26}N_3S_3In$ (435.39): C, 35.86; H, 6.02; N, 9.65; S, 22.09. Found C, 36.05; H, 6.04; N, 9.71; S, 22.16.

1,4,7-Tris(mercaptoethyl)-1,4,7-triazacyclodecyliron(III) (FeL2). H_3**L2**·3 HCl (0.25 mmol, 108 mg) was dissolved in anhydrous MeOH (10 mL), a few drops of diisopropylethylamine were added, and the mixture was heated to 60 °C. Then a solution of Fe(acac)$_3$ (0.25 mmol, 88 mg) in dry MeOH (5 mL) was added. The color of the solution changed to deep purple immediately, and a slow crystallization commenced. After several hours, the crystals were filtered off, washed with MeOH, and dried in vacuo. Yield: 40 mg (42%). MS (DEI+): m/z = 376 (M·$^+$). Anal. Calcd for $C_{13}H_{26}N_3S_3Fe$ (376.41): C, 41.48; H, 6.96; N, 11.60; S, 25.56. Found C, 41.46; H, 6.76; N, 11.00; S, 25.35. (Note: This synthesis can also be carried out using $FeCl_3 \cdot 6\ H_2O$, affording comparable yields.)

9-Methyl-1,4,7-tris(mercaptoethyl)-1,4,7-triazacyclodecane Trihydrochloride (H_3L3·3 HCl). 2 (70 mmol, 1.1 g) and ethylene sulfide (41 mmol, 2.5 g, 2.5 mL) were dissolved in toluene (50 mL) and stirred for 3.5 h at 50 °C. Then the solvents were evaporated in vacuo, and the crude product was dissolved in dry diethyl ether (100 mL). A small amount of insoluble compound was removed by filtration. Then a solution of dry HCl in ether was added dropwise with stirring, whereupon the title compound was obtained as a fine colorless precipitate. The solids were filtered off, washed with dry diethyl ether, and dried in vacuo to yield 3.0 g of a colorless powder. ^{1}H NMR (250 MHz, D_2O): δ = 0.88 [s, broad], 2.4−3.7 [m, broad] ppm. ^{13}C NMR (62.9 MHz, D_2O): 16.2 (broad), 18.2, 23.9, 31.1, 31.7, 35.2, 47−55 (broad), 55−63 (broad) ppm.

Table 5. Crystallographic Data

compound	Fe**L1**	Fe**L2**	Ga**L2**	In**L2**	Ga**L3**	In**L3**
formula	$C_{12}H_{24}N_3S_3Fe$	$C_{13}H_{26}N_3S_3Fe$	$C_{13}H_{26}N_3S_3Ga$	$C_{13}H_{26}N_3S_3In$	$C_{14}H_{28}N_3S_3Ga$	$C_{14}H_{28}N_3S_3In$
M/g mol^{-1}	362.37	376.40	390.27	435.37	404.29	449.39
T/°C	−90(2)	−90(2)	−90(2)	−90(2)	−90(2)	−90(2)
crystal system	monoclinic	monoclinic	monoclinic	monoclinic	monoclinic	monoclinic
space group	$P2_1/n$	$P2_1/c$	$P2_1/c$	$P2_1/c$	Cc	$P2_1/c$
a [Å]	7.2598(3)	7.7348(4)	7.7375(3)	7.8305(4)	9.4838(6)	14.5325(5)
b [Å]	16.6014(5)	14.5116(5)	14.4659(4)	14.5653(7)	14.3621(12)	7.3768(2)
c [Å]	12.8128(4)	14.5702(7)	14.5557(5)	14.8132(4)	12.9737(11)	16.8356(7)
β [deg]	93.967(2)	104.003(2)	103.934(2)	104.885(3)	102.070(5)	102.273(2)
V [Å^3]	1540.54(9)	1586.82(12)	1581.28(9)	1632.80(12)	1728.0(2)	1763.58(11)
Z	4	4	4	4	4	4
ρ [g cm^3]	1.562	1.576	1.639	1.771	1.554	1.693
μ [cm^{-1}]	13.76	13.39	21.3	18.25	19.52	16.93
measured data	10178	10474	11014	10878	5659	11573
data with $I > 2\sigma(I)$	2874	2660	2942	2725	2831	3351
unique data/R_{int}	3525/0.0336	3612/0.0473	3613/0.0383	3654/0.0514	3432/0.0537	4002/0.0379
wR_2 (all data, on F^2)[a]	0.0753	0.0890	0.0703	0.0856	0.0941	0.0683
R_1 $I > 2\sigma(I)$[a]	0.0289	0.0358	0.0293	0.0351	0.0463	0.0296
s[b]	1.010	1.007	1.025	1.004	1.026	1.011
res. dens. [e Å^3]	0.358/−0.396	0.371/−0.388	0.449/−0.456	0.615/−0.864	0.861/−0.965	0.538/−0.572
Flack-parameter					0.005(14)	
CCDC No.	716217	716216	716214	716215	716218	716219

[a] Definition of the R indices: $R_1 = \sum||F_o| - |F_c||/\sum|F_o|$; $wR_2 = \{\sum[w(F_o^2 - F_c^2)^2]/\sum w(F_o^2)^2\}^{1/2}$ with $w^{-1} = \sigma^2(F_o^2) + (aP)^2$. [b] $s = \{\sum[w(F_o^2 - F_c^2)^2]/(N_o - N_p)\}^{1/2}$.

MS (DEI+): 304 (100%, M•$^+$ − SH), 338 (65%, MH$^+$), 364 (24%, HS-Et-M•$^+$ − SH), 398 (20%, HS-Et-MH$^+$). Anal. Calcd for $C_{14}H_{31}N_3S_3$•3 HCl (447.00): C, 37.26; H, 7.67; N, 9.40; S, 21.52. Found C, 38.54; H, 5.88; N, 9.24; S, 22.68. *Note:* This data indicates the presence of an impurity, which according to mass spectrometric data is the product of insertion of one thiol moiety into ethylene sulfide. According to MS, its amount can be determined to be approximately 25%.

9-Methyl-1,4,7-tris(mercaptoethyl)-1,4,7-triazacyclodecylgallium(III) (GaL3). H_3**L3**•3 HCl (0.5 mmol, 223 mg) was dissolved in dry MeOH (100 mL). Then a solution of $Ga(NO_3)_3$•9 H_2O (0.5 mmol, 213 mg) was added very slowly at 60 °C. Upon addition, formation of a very fine precipitate (cloudiness of the solution) was observed, which dissolved after short time. Then the solution was refluxed for 30 min, and an excess of a solution of diisopropylethylamine in MeOH was added dropwise. A small amount of white precipitate was formed, which was filtered off. After standing overnight, a colorless precipitate formed in the solution, which was filtered off and recrystallized from DMF to yield 90 mg (45%) of the complex in form of clear prisms. MS (DEI+): m/z = 403, 405 (M•$^+$). Anal. Calcd for $C_{14}H_{28}N_3S_3Ga$ (404.32): C, 41.59; H, 6.98; N, 10.39; S, 23.79. Found C, 41.52; H, 6.99; N, 10.23; S, 23.61.

9-Methyl-1,4,7-tris(mercaptoethyl)-1,4,7-triazacyclodecylindium(III) (InL3). Anhydrous $InCl_3$ (0.5 mmol, 110 mg) was dissolved in 80 mL of a 0.1 M solution of NaOMe in MeOH. Then H_3**L3**•3 HCl (0.5 mmol, 216 mg) was added, whereupon a white amorphous solid was formed. This was filtered off, and the solution left standing for crystallization at 40 °C. A colorless precipitate was obtained, which was filtered off and recrystallized from dry DMF to yield 65 mg (29%) of the complex as clear prisms. MS (DEI): m/z = 449 (M•$^+$). Anal. Calcd for $C_{14}H_{28}N_3S_3In$ (449.42): C, 37.42; H, 6.28; N, 9.35; S, 21.41. Found C, 37.52; H, 6.28; N, 9.43; S, 21.59.

Crystal Structure Determination. The intensity data was collected on a Nonius KappaCCD diffractometer, using graphite-monochromated Mo−K(α) radiation. Data were corrected for Lorentz and polarization effects but not for absorption.[41−43] The structures were solved by direct methods (SHELXS)[44] and refined by full-matrix least-squares techniques against F_o^2 (SHELXL-97[45]). All non-disordered non-hydrogen atoms were refined anisotropically.[45] XP (SIEMENS Analytical X-ray Instruments, Inc.) was used for structure representations. The drawings in the paper were generated using PLATON.[46]

Table 6. Experimental (XRD) and Calculated Average Bond Distances [Å] of the Metal Coordination Environment of Ga**L1** Obtained with Different Basis Sets

	6-311G(d)	SBKJC/ 6-311G(d)	SDD/ 6-311G(d)	LanL2Dz/ 6-311G(d)	X-ray
Ga−S	2.34	2.34	2.37	2.36	2.34
Ga−N	2.41	2.43	2.42	2.36	2.21

(41) *Molen, an interactive structure solution procedure*; Enraf-Nonius: Delft, The Netherlands, 1999.
(42) *Collect, data collection software*; Nonius: The Netherlands, 1998.
(43) Otwinowski, Z.; Minor, W. In *Methods in Enzymology*; Carter, C. W., Jr., Ed.; Academic Press: New York, 1997; Vol. *276*, pp 307−326.
(44) Sheldrick, G. M. *Acta Crystallogr., Sect. A: Found. Crystallogr.* **1990**, *46*, 467–473.
(45) Sheldrick, G. M. *Shelxl-97*, release 97-2; University of Göttingen: Göttingen, Germany, 1997; http://shelx.uni-ac.gwdg.de/SHELX/ (accessed Jan 15, 2009).
(46) Spek, A. L. *Platon, a multipurpose crystallographic tool*; Utrecht University: Utrecht, The Netherlands, 2004; http://www.cryst.chem.uu.nl/platon (accessed Jan 15, 2009).
(47) Frisch, M. J.; Trucks, G. W.; Schlegel, H. B.; Scuseria, G. E.; Robb, M. A.; Cheeseman, J. R. ; Montgomery J.A. Jr.; Vreven, T.; Kudin, K. N.; Burant, J.C.; Millam, J. M.; Iyengar, S. S.; Tomasi, J.; Barone, V.; Mennucci, B.; Cossi, M.; Scalmani, G.; Rega, N.; Petersson, G. A.; Nakatsuji, H.; Hada, M.; Ehara, M.; Toyota, K.; Fukuda, R.; Hasegawa, J.; Ishida, M.; Nakajima, T.; Honda, Y.; Kitao, O.; Nakai, H.; Klene, M.; Li, X.; Knox, J. E.; Hratchian, H. P.; Cross, J. B.; Bakken, V.; Adamo, C.; Jaramillo, J.; Gomperts, R.; Stratmann, R. E.; Yazyev, O.; Austin, A. J.; Cammi, R.; Pomelli, C.; Ochterski, J. W.; Ayala, P. Y.; Morokuma, K.; Voth, G. A.; Salvador, P.; Dannenberg, J. J.; Zakrzewski, V. G.; Dapprich, S.; Daniels, A. D.; Strain, M. C.; Farkas, O.; Malick, D. K.; Rabuck, A. D.; Raghavachari, K.; Foresman, J. B.; Ortiz, J. V.; Cui, Q.; Baboul, A. G.; Clifford, S.; Cioslowski, J.; Stefanov, B. B.; Liu, G.; Liashenko, A.; Piskorz, P.; Komaromi, I.; Martin, R. L.; Fox, D. J.; Keith, T.; Al.Laham, M. A.; Peng, C. Y.; Nanayakkara, A.; Challacombe, M.; Gill, P. M. W.; Johnson, B.; Chen, W.; Wong, M. W.; Gonzalez, C.; Pople, J. A. *Gaussian 03*; Gaussian, Inc.: Wallingford, CT, 2004.

Computational Details. All calculations were performed using the Gaussian 03 program.[47] We employed the hybrid density functional B3LYP as implemented in Gaussian 03.[48,49] Structure optimizations without constraints of the M**L2** and M**L3** systems ($M = Ga^{3+}$, In^{3+}) were performed both in vacuo and in the presence of a dielectric continuum. We used the standard 6-311G(d) basis set for the ligand atoms and the LanL2DZ valence and effective core potential (ECP) functions for Ga and In.[50] This ECP has been demonstrated earlier to provide reliable results for different Ga^{3+} and In^{3+} complexes.[51−54] Test calculations performed in vacuo on the Ga**L1** system showed that the use of this combination of basis sets provides a reasonably good agreement of calculated and experimental (X-ray) structures. During these tests, we noticed that the use of the following basis sets exhibits a poorer performance (see Table 6): (i) the standard all-electron 6-311G(d) basis set for all atoms (including Ga); (ii) the standard 6-311G(d) basis set for the ligand atoms and the SBKJC VDZ valence and ECP functions of Stevens et al.[55] for Ga; (iii) the standard 6-311G(d) basis set for the ligand atoms and the Stuttgart-Dresden basis set (SDD)[56] and ECP for Ga.

Solvent effects were included by means of the integral equation formalism variant of the polarizable continuum model (IEF-PCM).[57,58] In line with the united atom topological model (UATM),[59] the solute cavity is built as an envelope of spheres centered on atoms or atomic groups with appropriate radii. Calculations were performed using an average area of 0.2 $Å^2$ for all the finite elements (tesserae) used to build the solute cavities. The stationary points found on the potential energy surfaces as a result of geometry optimizations in vacuo and in DMSO solution have been tested to represent energy minima rather than saddle points via frequency analysis. In solution relative Gibb's free energies of the different conformations of M**L2** and M**L3** complexes include both electrostatic and non-electrostatic contributions as well as zero point energy corrections obtained by frequency analysis. Cartesian coordinates for optimizations in vacuo and including solvent modeling for M**L2** and M**L3** systems ($M = Ga^{3+}$, In^{3+}) are given as Supporting Information.

NMR of Metal Complexes. NMR spectra of Ga**L2**, Ga**L3**, In**L2**, and In**L3** were measured with Varian Unity Inova 300 and Bruker Avance 400 spectrometers using samples containing 2−4 mg complex in 0.5 mL of DMSO-d_6. In all cases, the samples had to be heated to 60−70 °C to effect dissolution as at r.t. no sufficient amount of crystal material could be dissolved. A complete set of the spectra recorded for Ga**L2**, Ga**L3**, In**L2**, and In**L3** is given as Supporting Information.

For the experimental determination of the vicinal coupling constants of the propylene protons in complexes Ga**L2**, In**L2**, and In**L3**, exchange between enantiomeric forms $\Delta(\lambda\lambda)(\delta\delta\delta) \rightleftharpoons \Lambda(\delta\delta)(\lambda\lambda\lambda)$ was assumed to be fast on the ^{1}H NMR time scale. Therefore, the values of exchanging protons were averaged. The coupling constants for In**L3** were measured at room temperature with homonuclear decoupling at either the CH_3 protons or at H4. For Ga**L2** and In**L2**, the spectra were measured at 90 and 55 °C, respectively, because then the resonances were sharp and the exchange between the isomers was fast on the ^{1}H NMR time scale. Signal assignments were supported by COSY and one-dimensional TOCSY spectra (see Supporting Information).

Acknowledgment. Thanks are due to the EU for financial support via a Marie Curie training site host fellowship (QLK5-CT-2000-60062). This work was done in the frame of COST Action D38 Metal-Based Systems for Molecular Imaging Applications and the EU Network of Excellence European Molecular Imaging Laboratories (EMIL, LSCH-2004-503569). The authors are indebted to Centro de Computacion de Galicia for providing the computer facilities. J.N. gratefully acknowledges financial support through a postdoctoral grant from the DAAD (German Academic Exchange Service).

Supporting Information Available: NMR spectra for the complexes Ga**L2**, In**L2**, Ga**L3**, and In**L3**, Cartesian coordinates for all DFT-optimized structures are provided. This material is available free of charge via the Internet at http://pubs.acs.org. Also, the crystallographic data (excluding structure factors) has been deposited with the Cambridge Crystallographic Data Centre as supplementary publication CCDC-716214 for Ga**L2**, −716215 for In**L2**, −716216 for Fe**L2**, −716217 for Fe**L1**, −716218 for Ga**L3**, and −716219 for In**L3**. Copies of the data can be obtained free of charge on application to CCDC, 12 Union Road, Cambridge CB2 1EZ, U.K. [e-mail: deposit@ccdc.cam.ac.uk].

IC900119A

(48) Stephens, P. J.; Devlin, F. J.; Chabalowski, C. F.; Frisch, M. J. *J. Phys. Chem.* **1994**, *98*, 11623–11627.
(49) Scuseria, G. E.; Staroverov, V. N. In *Theory and Applications of Computational Chemistry: The First Forty Years*; Dykstra, C. E.; Frenking, G.; Kim, K. S.; Scuseria, G. E., Eds.; Elsevier: Amsterdam, 2005; Chapter 24, pp 669−724.
(50) Wadt, W. R.; Hay, P. J. *J. Chem. Phys.* **1985**, *82*, 284–298.
(51) Narbutt, J.; Czerwiński, M.; Krejzler, J. *Eur. J. Inorg. Chem.* **2001**, 3187–3197.
(52) Lau, E.; Lightstone, F.; Colvin, M. *Inorg. Chem.* **2006**, *45*, 9225–9232.
(53) Song, Y.-H.; Chiu, Y.-C.; Chi, Y.; Chou, P.-T.; Cheng, Y.-M.; Lin, C.-W.; Lee, G.-H.; Carty, A. J. *Organometallics* **2008**, *27*, 80–87.
(54) Thoi, V.; Stork, J.; Magde, D.; Cohen, S. *Inorg. Chem.* **2006**, *45*, 10688–10697.
(55) Stevens, W. J.; Krauss, M.; Basch, H.; Jasien, P. G. *Can. J. Chem.* **1992**, *70*, 612.
(56) Bergner, A.; Dolg, M.; Küchle, W.; Stoll, H.; Preuss, H. *Mol. Phys.* **1993**, *80*, 1431–1441.
(57) Barone, V.; Cossi, M.; Tomasi, J. *J. Chem. Phys.* **1997**, *107*, 3210–3221.
(58) Tomasi, J.; Mennucci, B.; Cammi, R. *Chem. Rev. (Washington, DC, U.S.)* **2005**, *105*, 2999–3093.
(59) Peng, C.; Ayala, P. Y.; Schlegel, H. B.; Frisch, M. J. *J. Comput. Chem.* **1996**, *17*, 49–56.